

PAPER • OPEN ACCESS

First clinical implementation of a highly efficient daily online adapted proton therapy (DAPT) workflow

To cite this article: F Albertini *et al* 2024 *Phys. Med. Biol.* **69** 215030

You may also like

- [Opportunities and challenges of upright patient positioning in radiotherapy](#)
Lennart Volz, James Korte, Maria Chiara Martire *et al.*
- [Experimental validation of daily adaptive proton therapy](#)
Lena Nenoff, Michael Matter, Marjolaine Charmillot *et al.*
- [Modelling radiobiology](#)
Lydia L Gardner, Shannon J Thompson, John D O'Connor *et al.*

View the [article online](#) for updates and enhancements.



physicsworld WEBINAR

ZAP-X radiosurgery & ZAP-Axon SRS planning

Technology Overview, Workflow, and Complex Case Insights from a Leading SRS Center

Get an inside look at European Radiosurgery Center Munich – a high-volume ZAP-X centre – with insights into its vault-free treatment suite, clinical workflow, patient volumes, and treated indications. The webinar will cover the fundamentals of the ZAP-X delivery system and what sets it apart from other SRS platforms; showcase real-world performance through complex clinical cases; and provide a concise overview of the recently unveiled next-generation ZAP-Axon radiosurgery planning system.

LIVE at 4 p.m. GMT/8 a.m. PST, 19 Feb 2026

[Click to register](#)



OPEN ACCESS

RECEIVED
15 May 2024REVISED
29 July 2024ACCEPTED FOR PUBLICATION
18 September 2024PUBLISHED
11 November 2024

Original content from this work may be used under the terms of the Creative Commons Attribution 4.0 licence.

Any further distribution of this work must maintain attribution to the author(s) and the title of the work, journal citation and DOI.



Physics in Medicine & Biology

IPEM
Institute of Physics and
Engineering in Medicine**PAPER**

First clinical implementation of a highly efficient daily online adapted proton therapy (DAPT) workflow

F Albertini^{1,*} K Czerska¹, M Vazquez¹, I Andaca¹, B Bachtary¹, R Besson¹, A Bolsi¹, A Bogaert¹, E Choulilitsa^{1,2} J Hrbacek¹, S Jakobsen¹, D Leiser¹, M Matter¹, A Mayor¹, G Meier¹, A Nanz¹, L Nenoff¹, D Oxley¹, D Siewert¹, B A Rohrer Schnidrig¹, A Smolders^{1,2} H Szweda¹, M Van Heerden¹, C Winterhalter¹, AJ Lomax^{1,2} and DC Weber^{1,3}

¹ Center for Proton Therapy- Paul Scherrer Institute, Villigen, Switzerland

² Department of Physics, ETH Zurich, Zurich, Switzerland

³ Department of Radiation Oncology, Inselspital, Bern University Hospital and University of Bern, Bern, Switzerland

* Author to whom any correspondence should be addressed.

E-mail: francesca.albertini@psi.ch

Keywords: DAPT, daily adaptive proton therapy, online adaptive proton therapy, adaptive proton therapy

Abstract

Objective. This study presents the first clinical implementation of an efficient online daily adaptive proton therapy workflow (DAPT). **Approach.** The DAPT workflow includes a *pre-treatment phase*, where a *template* and a *fallback plan* are optimized on the planning computed tomography (CT). In the *online phase*, the *adapted plan* is re-optimized on daily images from an in-room CT. Daily structures are rigidly propagated from the planning CT. Automated Quality Assurance (QA) involves geometric, sanity checks and an independent dose calculation from the machine files. Differences from the template plan are analyzed field-by-field, and clinical plan is assessed by reviewing the achieved clinical goals using a traffic light protocol. If the daily adapted plan fails any QA or clinical goals, the fallback plan is used. In the *offline phase* the delivered dose is recalculated from log-files onto the daily CT, and a gamma analysis is performed (3%/3 mm). The DAPT workflow has been applied to selected adult patients treated in rigid anatomy for the last serie of the treatment between October 2023 and April 2024. **Main Results.** DAPT treatment sessions averaged around 23 min [range: 15–30 min] and did not exceed the typical 30 minute time slot. Treatment adaptation, including QA and clinical plan assessment, averaged just under 7 min [range: 3:30–16 min] per fraction. All plans passed the online QAs steps. In the offline phase a good agreement with the log-files reconstructed dose was achieved (minimum gamma pass rate of 97.5%). The online adapted plan was delivered for >85% of the fractions. In 92% of total fractions, adapted plans exhibited improved individual dose metrics to the targets and/or organs at risk. **Significance.** This study demonstrates the successful implementation of an online daily DAPT workflow. Notably, the duration of a DAPT session did not exceed the time slot typically allocated for non-DAPT treatment. As far as we are aware, this is a first clinical implementation of daily online adaptive proton therapy.

1. Introduction

Proton therapy using pencil beam scanning (PBS) is a rapidly expanding radiotherapy modality, with more than 130 treatment facilities worldwide providing to cancer patients this delivery paradigm, as reported by the (2024). The well-defined range of the proton Bragg peak can be however considered a two-edged sword. On one side, it allows for highly conformal doses to the target, with substantial reduction of doses to surrounding normal tissues, whilst on the other, the accuracy of delivery is sensitive to uncertainties in the precise position and shape of the proton radiation peak in the patient. Many factors contribute to such uncertainties, ranging from residual patient misalignments, through inherent uncertainties in the computed tomography (CT) data used for calculating range *in vivo*, to inter-fractional anatomical changes that can

occur over the duration of the treatment course (Lomax 2008, Paganetti 2012, Paganetti *et al* 2021). For CT uncertainties, the use of dual energy CT is becoming more prevalent, which in many anatomical regions can substantially reduce CT induced range uncertainties (Li *et al* 2017, Peters *et al* 2022, Taasti *et al* 2023). In addition, to compensate for potential CT and positional uncertainties, robust optimization during treatment planning is now the standard of care in PBS proton therapy (Unkelbach *et al* 2018, Korevaar *et al* 2019, Janson *et al* 2024). This has been shown to improve plan robustness also against moderate anatomical variations but at the cost of increased normal tissue dose (Jagt *et al* 2020, Lalonde *et al* 2021). However, its ability to compensate for major anatomical changes is limited, particularly as the magnitude and location of such changes is difficult to predict *a priori* (Cubillos-Mesías *et al* 2019, Jagt *et al* 2020, Lalonde *et al* 2021, Paganetti *et al* 2021).

One of the most effective methods for dealing with anatomical changes during treatment could however be adaptive therapy based on regular re-imaging and re-planning during the course of the patient's treatment. The concept of regular treatment adaption in radiotherapy was first proposed by Yan *et al* in their seminal paper from 1997 (Yan *et al* 1997). Although offline adaption (re-planning patients between fractions) has been practiced for many years, the concept of online adaption (Albertini *et al* 2020), whereby the patient remains on the couch during the adaptive process, has been slow to come into the clinic. This has recently changed in photon-based radiotherapy with the introduction of dedicated MR and CBCT based, integrated Linac systems which have been specifically designed for online adaptive therapy (Acharya *et al* 2016, Papalazarou *et al* 2017, Raaymakers *et al* 2017, Winkel *et al* 2019, Glide-Hurst *et al* 2021).

Such technological developments indicate the importance and clinical interest in regular and frequent treatment adaption. In the photon setting, such adaptions are mainly driven by day-to-day changes in tumor position and shape (defined here as ‘tumour driven’ adaption), and less by anatomical changes in the normal tissues and structures in the beam path to the tumor (‘anatomy driven’). For proton therapy however, both are important, meaning that regular adaptive therapy is likely even more important and necessary than in photon radiotherapy (Albertini *et al* 2020, Paganetti *et al* 2021, Chang *et al* 2024) due to the conformality of proton radiation dose deposition (i.e. Bragg Peak). Indeed, as has previously been demonstrated in planning studies, ‘anatomy driven’ adaption in proton therapy can even improve the quality of the adapted dose distribution in comparison to the original treatment plan, by exploiting advantageous anatomical situations such as reduced density heterogeneities (Nenoff *et al* 2019) or improved separation between the target and organs at risk.

Moreover, considering that residual set-up errors, such as translations and/or rotations of the patient, can significantly impact proton range, implementing a daily “up-front⁴” anatomical adaptation approach based on a ‘CT-of-the-day’ paradigm during treatment could effectively minimize safety margins compared to non-daily adapted delivery methods (Nenoff *et al* 2019, Lalonde *et al* 2023, Oud *et al* 2024).

In this paper, we report on the first ‘in-patient’ demonstration of a highly efficient, up-front and online adaptive proton therapy workflow that has been developed and clinically implemented at our institute. As far as we are aware, this is the first clinical implementation of an online adapted therapy for proton therapy. Our workflow has been applied for limited numbers of fractions to five patients treated with tumors in the brain or skull-base region. For all patients, individual steps of the DAPT workflow have been timed and documented, the delivered dose has been evaluated using log-based dose reconstruction for all delivered and adapted fractions. In addition, although not part of the regular DAPT workflow, all adapted plans have been retrospectively measured.

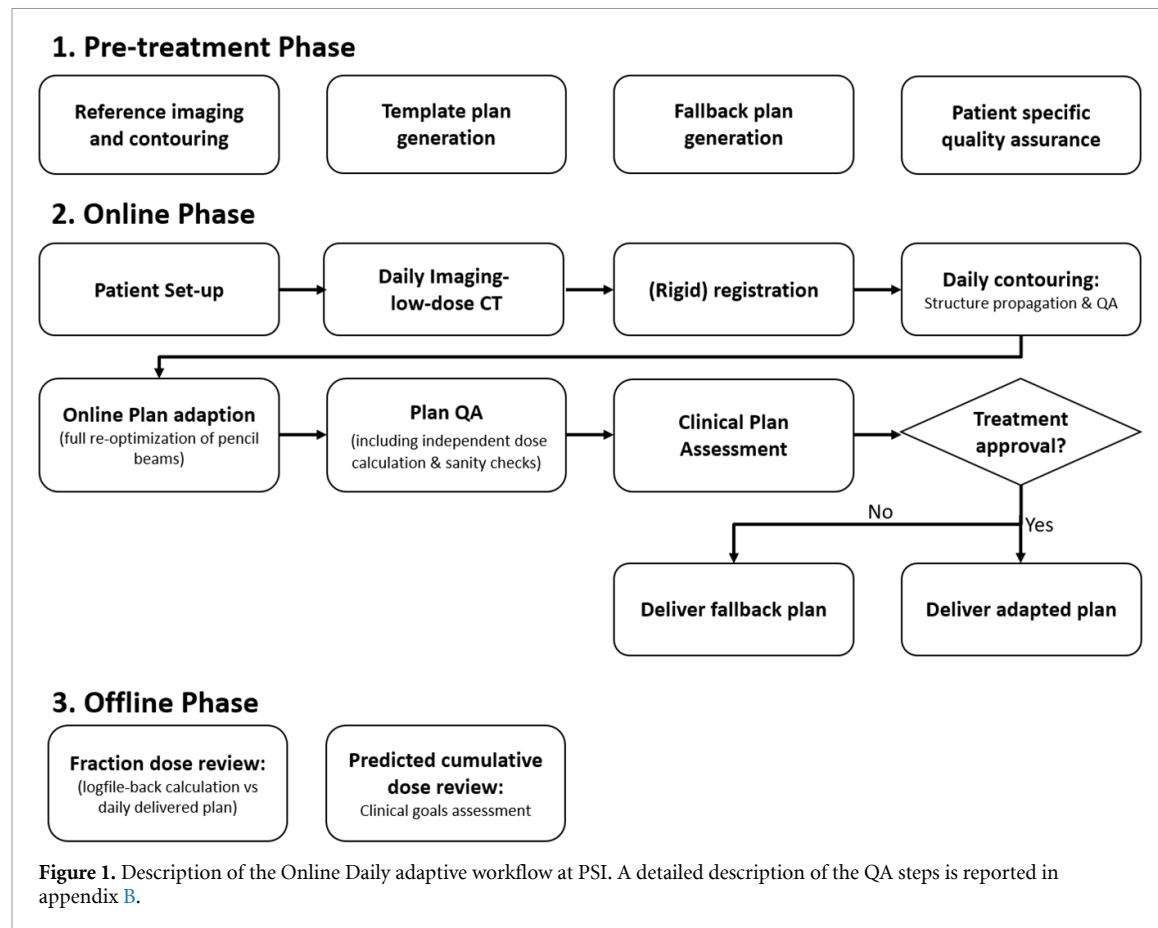
2. Materials and methods

2.1. DAPT workflow and automated QA

The daily adapted proton therapy workflow developed at our institute is shown in figure 1, and has been previously described in detail, as well as extensively tested on phantoms (Matter 2020, Nenoff *et al* 2021).

In short, in the **pre-treatment phase**, a reference plan, referred to as the ‘template plan,’ and a back-up plan, referred as ‘fallback plan’ are optimized on the planning CT (Somatom Sensation Open, Siemens Healthcare GmbH, Erlangen, Germany, with a pixel size of 0.97 mm*0.97 mm) and undergo conventional (i.e. non-DAPT) clinical and treatment approval steps, such as the assessment of clinical goals, and patient specific quality assurance, including the measurement of the two plans (Lomax *et al* 2004, Albertini *et al* 2015). These plans are entirely independent of each other, potentially utilizing different beam arrangements and optimization parameters. The template plan serves as a reference for the online optimized plan, while the fallback plan represents the strategy for a non-adapted delivery and can be selected on any day as an

⁴ Daily ‘up-front’ adaptation: always adapt every day, as recently defined by the EPTN (European Proton Therapy Network) Task Group on Adaptive Proton Therapy



alternative providing it is necessary. In the initial clinical implementation discussed here, these two plans have been intentionally kept identical.

In the **online phase**, for each fraction, a daily CT (Somatom Sensation Open, Siemens Healthcare GmbH, Erlangen, Germany, with a pixel size of 0.97 mm*0.97 mm) is acquired with the patient on the treatment couch, using a low-dose protocol (120 kV, quality reference mAs: 20, care dose, pitch 1, rotation time 0.5 s), on a diagnostic quality, in-room CT-on-rails (figure 2). This has been calibrated to proton stopping power with the same precision and accuracy as that used for all planning CT's at our institute as described elsewhere (Nenoff *et al* 2021) and in appendix A. After rigidly registering this 'image-of-the-day' to the original planning CT (see 'Patient selection' below), all structures are propagated from the planning CT to the daily CT, after which a fully automated re-optimization of the plan is performed using exactly the same field geometry and optimization objectives as for the template plan. As described by Matter *et al* (2019), for this we use a ray casting based analytical dose algorithm in order to ensure minimal optimization times. Simultaneously, an automated plan QA procedure is started which, amongst other things, checks the geometric accuracy of the rigidly propagated structures to the daily CT (see appendix B). Once the plan-of-the-day has been optimized and calculated, the dose distribution is compared to that of the template plan. Efficiency in this evaluation process is achieved by establishing tolerances for acceptable dose deviations (e.g. acceptable daily deviations from those achieved in the template plan of mean, min, max doses etc). This groundwork is done by the responsible radiation oncologist (MD) in the *pre-treatment phase* and is documented in the *DAPT daily acceptance table*. These variations aid in evaluating the online adapted plan, employing a traffic light protocol with the following color scheme:

- Green: Indicates a value equal to or better than accepted in the template plan.
- Yellow: Represents a value worse than the template plan, yet within the specified tolerance.
- Red: Indicates a value worse than the accepted template value, exceeding the defined tolerance.

In addition, and in parallel, an automated plan QA procedure is executed, based on an independent dose calculation using as its input information from the machine control file generated from the daily plan (Meier *et al* 2015, Scandurra *et al* 2016, Belosi *et al* 2017). This has previously been demonstrated to be an extremely sensitive method for checking the integrity of the transformation of treatment planning data to the machine



Figure 2. Gantry 2 treatment room at PSI equipped with a diagnostic quality, in-room CT-on-rails to enable online adaptive proton therapy. This setup allows for seamless transfer of the patient from the CT position to the treatment position under the gantry.

control system, and a check that is substantially more sensitive than experimental verifications at picking up potential errors in this transformation (Matter *et al* 2018).

Upon the approval of the daily structure by the responsible MD and the assessment of clinical goals, the decision-making criteria for the application of the daily plan are based on the plan QA checks. If the QA passes the daily adapted plan is delivered, if it fails the fallback plan is applied instead. Details on the full online QA process and of the used tolerances for DAPT can be found in the supplement to this paper (appendix B, Table 5, 6). To ensure that the correct plan is used for treatment, our oncology information system (OIS) has been modified to require daily approval of a treatment plan. This means that based on the daily decision, only one plan is promoted to be valid for delivery on that day.

In the **offline phase**, the dose delivered in each fraction is evaluated by automatically recalculating the dose on the daily anatomy using the log-files. This method, as previously described, provides the most accurate quality assurance assessment of the dose delivered to the patient on a daily basis (Matter *et al* 2018, Winterhalter *et al* 2019, Matter *et al* 2020, Nenoff *et al* 2021) and is performed with our in-house developed treatment planning system (TPS). The agreement between the planned and the delivered dose is assessed by performing a global gamma analysis with a dose/ distance passing criteria of 3%/ 3 mm. More information is reported in appendix B. Subsequently, the fulfillment of clinical goals is assessed based on the predicted cumulative dose. This cumulative dose is performed by combining the delivered daily doses (i.e. the dose reconstructed from the log-files) propagated on the reference image (i.e. the planning CT) using the inverse rigid transformations determined in the registration step of each fraction with the planned dose for the remaining fractions. For simplicity, the doses are accumulated physically, i.e. without biological correction, since the effect of such corrections is negligible if daily dose variations are small (Bortfeld and Paganetti 2006), as expected for the cases studied in this work. Moreover, even for the low-dose areas in lung cancer, where daily dose variations are generally larger than for tumors in the head, the effect of biological correction was found to be minor (Smolders *et al* 2023b).

2.2. Gantry 2 room and TPS

The described DAPT workflow has been implemented in the Gantry 2 room in our institute (see figure 2). Gantry 2 (Pedroni *et al* 2004) is a PBS machine with an upstream energy selection design and fast, double parallel scanning, with beam widths between 2.5 and 4.5 mm σ in air across the 70–230 MeV energy (Pedroni *et al* 2011). An electronically controlled range-shifter of 4 cm water-equivalent thickness is mounted within the nozzle and can be remotely positioned on a spot-by-spot basis into the beam to allow the delivery of Bragg peaks close to the patient surface.

The Gantry 2 room is equipped with an in-room CT and patients are treated with the in-house developed TPS since 2013 (Albertini *et al* 2015). This TPS is based on PSIplan, the first TPS developed ever for PBS proton therapy in 1996 (Lomax *et al* 1996). Our TPS uses the ray-casting dose calculation (Schaffner *et al* 1999), and a quasi-Newtonian fluence optimization algorithm (Lomax 1999).

To accelerate dose computation and optimization, these algorithms, along with other steps in the plan generation process, have been recently implemented onto dedicated GPU kernels using Java (Oracle Corporation, Redwood Shores, CA, USA). The GPU implementation is described elsewhere (Matter *et al* 2019).

Furthermore, to ensure the preservation of plan quality under conditions of changing patient geometry, the optimization algorithm was modified by implementing an iteratively changing dose volume histogram (DVH) constraint importance. In short, in each iteration, the relative importance γ of an OAR-DVH constraint increases if the constraint is not met, or decreases if it is met:

$$\gamma(k+1) = \gamma(k) \frac{D(k)}{C}.$$

Here, $D(k)$ is the dose at the specific OAR dose volume constraint at iteration k , and C is the constraint dose. The target's importance remains constant, ensuring target coverage is not enforced by the optimizer. Further information regarding the enforced optimization algorithm can be found elsewhere (Matter 2020, Nenoff *et al* 2021).

The upgraded version of the TPS (i.e. Flexible ION-planning Application -FIONA TPS), which includes the GPU implementation and the enforced constrained optimization algorithm has been in clinical use since 2021.

The DAPT workflow primarily integrates the commercial imaging system with the FIONA TPS and the in-house developed OIS into a dedicated engine called @DAPT. This engine was developed specifically to guide the steps in the online adaptive phase and has been comprehensively tested and commissioned before clinical use (Nenoff *et al* 2021).

2.3. Patient selection

In this initial phase of clinical implementation, 5 patients were selected for DAPT delivery, treated in the period between October 2023 and April 2024. To minimize risks with the introduction of such a workflow, the following criteria for patient selection, and constraints on the use of DAPT, have been defined for this initial phase:

1. Only tumours in rigid anatomical regions were selected (e.g. brain, skull base)
2. Only last series treatments of a patient's full treatment course were delivered using DAPT, so called 'DAPT serie'. Thus is, DAPT was delivered for the last consecutive 3–8 fractions, depending on the dose prescribed to the boosted volume (see table 1 below).
3. Pediatric patients were excluded.
4. Standard field arrangements and clinical safety margins were used. No set-up margin reduction has been implemented.
5. *Template* and *fallback* plans were kept the same.

Note, these selection criteria and constraints are not restrictive measures but rather serve the purpose of demonstrating the proof-of-principle and ensuring clinical safety of our DAPT workflow. It is important to note that these criteria are not optimized to fully exploit the potential clinical benefits of our approach. As our implementation progresses and matures, we anticipate refining these criteria to maximize the clinical advantages offered by DAPT.

2.4. Treatment plans and patient population

Plans were calculated on the images acquired with the in-room CT (, with the in-house developed TPS FIONA on a 3.5 mm*3.5 mm*3.5 mm voxel grid, with a 4 mm spot and between 2.5–5 mm Energy spacing. Plans were optimized using the CTV-to-PTV margins (see table 1) with a single field optimization (SFO) or a multi field optimization (MFO) technique to achieve the prescribed clinical goals based on clinical protocols.

For all patients, tumour indication, fraction dose, total number of fractions and the number of fractions delivered using the DAPT paradigm are shown in table 1. Also included are the number of fields of the DAPT plans and safety margins used. Example dose distributions calculated for each patient on the planning CT are shown in figure 3.

2.5. Workflow and clinical evaluations

For each DAPT fraction for each patient, times for the major workflow steps of the @DAPT workflow (see table 2) were recorded, together with the total duration of each fraction, defined as the time from the patient mounting the treatment couch to the patient dismounting, thus representing the effective occupancy of the

Table 1. Summary of the treated patients and treatment/planning characteristics. It includes the total number of fractions for the treatment, the number of fractions in the series plan scheduled with the DAPT workflow, and the number of DAPT-delivered fractions.

P #	Indication	Dose/fr [Gy(RBE)]	# fractions (treatment)	# fr DAPT serie [delivered] (%) total fraction)	# fields (Gantry & Couch)	Margins [mm]
P1	Hemangiopericytoma	1.8	33	5 [4] (12%)	2 (G160°, C180°, G160°, C0°)	PTV = GTV + 4 mm
P2	Chondrosarcoma of the skull base	2.0	35	8 [7] (20%)	3 (G70°, C150°, G120°, C150°, G70°, C10°)	PTV = CTV + 4 mm
P3	Ewing sarcoma (brain)	1.8	30	5 [4] (13%)	3 (G20°, C165°, G110°, C165°, G60°, C135°)	PTV = CTV + 4 mm
P4	Meningioma	1.8	33	3 [3] (9%)	2 (G85°, C165°, G125°, C165°)	PTV = CTV + 4 mm
P5	Giant Cell tumor of bone	1.8	30	5 [4] (13%)	3 (G110°, C165°, G80°, C165°, G90°, C15°)	PTV = CTV + 4 mm

Table 2. Report of time slots needed for the adaptive workflow averaged over all the fractions, including the daily CT acquisition and the treatment delivery. Note: the step of ‘image registration and verification’ is not an extra step of the online adaptive workflow, as this is also performed for the non-adaptive workflow to calculate the vectors to correct daily misalignments.

		Average duration [min-max] (min)
Set-up and CT acquisition		2:10 [1:00–8:10]
Online adaptive steps	Image registration and verification	4:10 [2:30–7:30]
	Initial integrity checks	1:00 [0:30–2:20]
	Daily structure approval	2:30 [0:50–10:40]
	Daily Plan clinical evaluation & approval	2:30 [0:40–4:50]
	Plan QA (incl. check of secondary dose)	0:50 [0:20–2:20]
Delivery		9:20 [6:00–14:00]
Total		23:20 [15:00–30:00]

treatment room. For clinical evaluation of the DAPT fractions, all online-adapted plans were retrospectively compared to the template plan.

For comparison, the dose of the non-adapted plan was also calculated on the daily CT’s, to estimate what would have been delivered to the patient if no daily adaption had been performed. The difference between the relevant dosimetric metrics (e.g. CTV V95%) in the adapted and non-adapted plans was calculated and a two-sided Wilcoxon signed rank test was included to test for significance ($p < 0.05$). Residual inaccuracies in the mechanical movements and patient motion after CT acquisition were neglected.

As each plan-of-the-day is calculated using an analytical dose calculation in the @DAPT workflow, all doses were also retrospectively re-calculated using the FRED Monte Carlo code (Schiavi *et al* 2017). Similarly, all daily plans were retrospectively experimentally verified and evaluated using the procedures and tolerances typically adopted at our institute. Finally, imaging doses resulting from the daily, low-dose CT acquisitions were estimated using standard CTDI approaches (see table 3).

3. Results

3.1. DAPT delivery

The template plans for all patients are shown in figure 3. For the DAPT series, the online adapted plans were selected in $>85\%$ of the DAPT fractions (22 from 26). For 3 fractions, the fallback plan was selected due to a

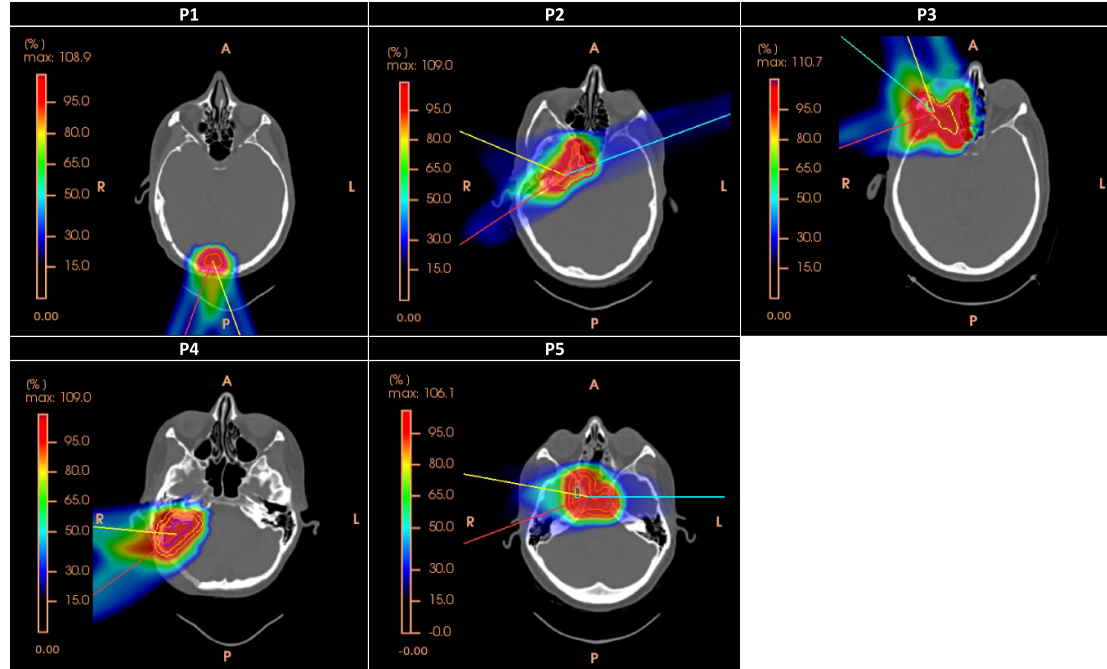


Figure 3. Dose distributions of the template plans and field arrangements for the 5 patients treated with the DAPT workflow.

Table 3. Imaging Dose (CTDI) of the planning CT (pCT) and of the daily low-dose CT for a single fraction (dCT).

P #	Imaging dose (CTDI)	
	pCT [mGy]	dCTs [mGy]
P1	18.77	4.61
P2	18.89	3.47
P3	21.77	3.27
P4	17.87	3.54
P5	17.97	3.5

marginal increase of 1% in the dose of a single critical structure, whereas for 1 fraction, the fallback plan was utilized due to a miscommunication in the clinical team (table 1). In addition, all adapted plans passed online QA, as well as post-treatment experimental verification with >96.6% agreement at the 3%/3 mm level.

Over all patients and fractions, the average duration of a DAPT fraction was just above 23 min [range: 15–30 min], of which the average time for delivery was 9 min [range: 6–14 min] (table 2). This is only slightly longer than a non-DAPT session, which for the same patients averaged just below 19 min [range: 13–49 min].

Treatment adaption, including plan and the assessment of clinical goals took on average just under 7 min per fraction.

Based on CTDI measurements of imaging dose, the additional acquisition of a daily low-dose CT image for 5 fractions resulted in a cumulative imaging dose lower than the acquisition of a weekly control-CT acquired with a standard protocol (table 3).

3.2. Clinical evaluation

The daily adapted plans yielded CTV and PTV coverage (V95%) within 1.1% of the planned dose and mostly improved the minimum dose (figure 4). However, the deviations in V95% and improvements in Dmin were not significantly different from what a conventional approach, i.e. the fallback plan recalculated on the daily anatomy, would have delivered. Indeed, a non-DAPT delivery could have resulted in a significantly larger Dmax, both to the targets and the OARs. More specifically, if the irradiation with the fallback plan had been chosen, it would have resulted in an increase of up to 10% in the brainstem dose for one patient. In contrast, the adaptive approach ensured that OAR doses were within the 5% threshold for *all fractions*. Results for the individual patients are reported in figures 8–12 in the Appendix C.

As an example, the template, daily and fallback plans for one fraction of patient 4 are shown in figures 5(a)–(c) together with the clinical goals and comparative DVH's (figures 5(d) and (e)).

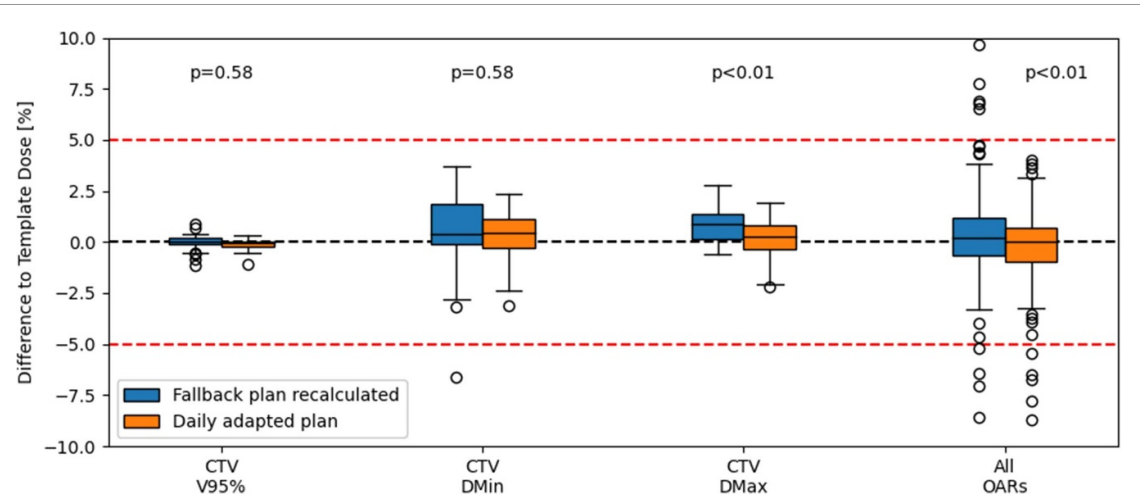


Figure 4. Deviations in daily dose metrics from the planned value for both the fallback and adapted plans ('fallback—template' and 'daily adapted—template'). The results include all patients. A difference larger than '0' indicates that the daily plans (either adapted or recalculated) deliver more dose than the template plan. The dose differences in all OARs used to guide the daily decision are combined in the 'All OARs' category. The individual results for each patient and OAR are shown in the appendix C. The p-values indicate for each dose metric the result of a wilcoxon signed rank test between the deviations of the conventional and adapted plan. Difference in the target Dmax and in the OARs are statistically different.

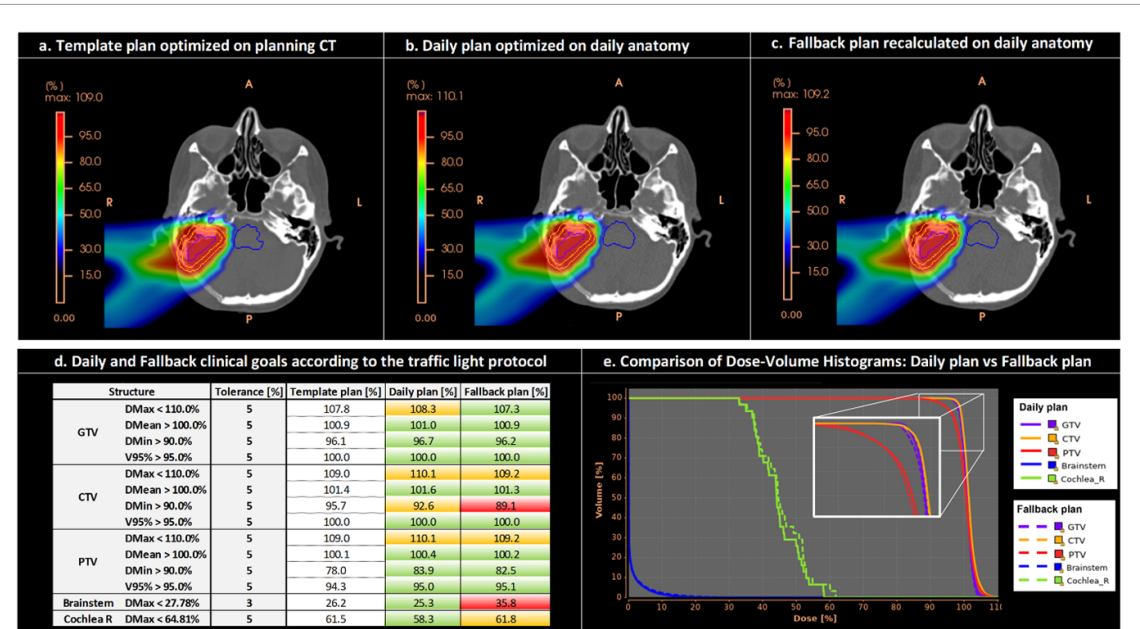


Figure 5. Example of dose distributions, clinical goals and DVHs for one fraction of patient 4. (a)–(c): Display of the template plan optimized on planning CT, the daily plan re-optimized on the daily anatomy, and the fallback plan recalculated on the daily anatomy. (d) Clinical goals of daily and fallback plans according to the traffic light protocol, with the following color scheme: Green: Indicates a value equal to or better than accepted in the template plan. Yellow: Represents a value worse than the template plan but with a deviation smaller than the tolerance. Red: Indicates a value worse than the accepted template value, with the deviation larger than the tolerance (e) comparative DVHs of the relevant structures for daily and fallback plans.

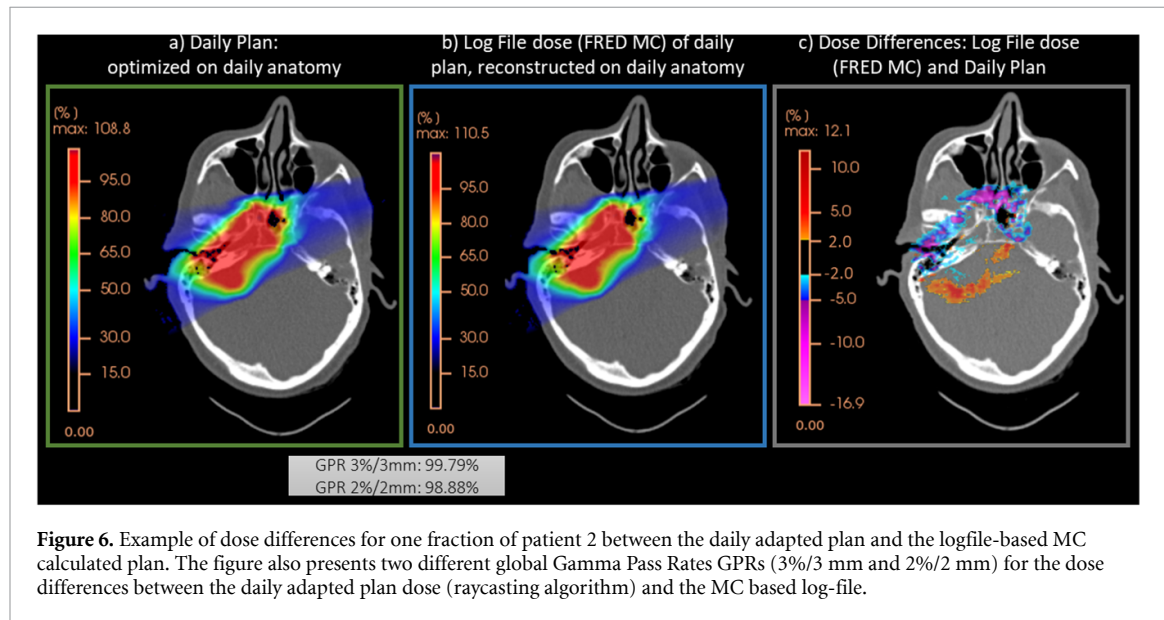
Finally, good agreement was also achieved between the online optimized plan and the logfile-based Monte Carlo dose calculation. Indeed, over all the fractions, more than 97.5% of voxels met the gamma analysis criteria of 3% / 3 mm, while more than 89% adhered to the stricter 2%/2 mm criteria (table 4). Figure 6 illustrates an example for one fraction of patient 2.

4. Discussion

This study demonstrates the successful clinical implementation of an efficient online daily adapted proton therapy workflow for brain/skull base tumor patients treated with proton therapy. Notably, the duration of a DAPT session was on average just above 23 min and did not exceed the timeslot typically allocated for a non-DAPT treatment. In fact, for these patients, the DAPT session was only marginally longer than the

Table 4. Comparison between the DAPT plan optimized daily with a ray casting algorithm and the dose reconstructed with a MC dose calculation algorithm from the log-file. The agreement is analyzed on voxels receiving >10% of the prescribed dose. Global Gamma Pass Rate are reported on average [range] for two different dose/distance levels.

P #	Agreement between DAPT plan and log-file based MC dose	
	Gamma Pass Rate (3%/3 mm)	Gamma Pass Rate (2%/2 mm)
P1	100% [99.9%–100%]	98.6% [98.3%–98.7%]
P2	99.8% [99.7%–99.8%]	98.7% [98.7%–98.9%]
P3	98.3% [97.5%–99.8%]	89.5% [89.0%–90.1%]
P4	99.0% [98.5%–99.3%]	95.0% [94.9%–95.2%]
P5	99.9% [99.7%–100%]	99.6% [99.6%–99.7%]



equivalent non-DAPT sessions (average, 19 min). For non-DAPT treatment, the time required for positioning the patient could indeed be longer. And, in case of suboptimal positioning, a repositioning occurs, thus extending the treatment time (i.e. the time of the gantry occupancy).

In our initial phase of implementation, we have deliberately focused on patients with tumors located in rigid anatomical regions, such as the brain and skull base, and started DAPT delivery only for a limited number of fractions and using the same planning approach (setup uncertainties i.e. CTV-to-PTV margins and beam arrangements) as for non-DAPT treatments. This cautious approach aimed to ensure patient safety while demonstrating the feasibility of our workflow. As a next step, we aim to capitalize the advantage of DAPT for rigid anatomy by including the delivery of a full DAPT treatment (i.e. all fractions), margin reduction, and potentially using more conformal beam angles. These advances promise to optimize treatment outcomes while minimizing unnecessary radiation exposure to healthy tissues (Nenoff *et al* 2019, Oud *et al* 2024). For such extensions, our currently implemented workflow can be used without modification. The DAPT workflow supports the use of two different plans: a template plan that could be optimized with reduced margins and potentially a more conformal beam configuration, and a fallback plan to be optimized with conventional planning settings. Moreover, the efficiency of the DAPT treatment is expected to be maintained because, with the implemented daily up-front adaptation, the plan is always adapted on a daily basis to the daily image. Thus, the additional burden of performing an initial plan comparison to assess the need for online adjustment will be eliminated.

A key further extension for DAPT is to enable the same efficient adaptive treatment with non-rigid anatomical regions. One of the critical missing elements to minimize the extra time needed for online adaptation is the development of a fast review and approval protocol for the daily structures, even in the presence of deforming anatomy. Indeed, the time required to review automatically segmented and propagated structures remains one of the bottlenecks in online adaptive workflows for systems such as the MRI Linac and ETHOS (van Herk *et al* 2018, Winkel *et al* 2019, Werenstein-Honingh *et al* 2019, Byrne *et al* 2022, Güngör *et al* 2000), thus possibly limiting the wider adoption of online adaptive treatment.

A recent study suggests that, when the dosimetric impact of residual contour uncertainties are included in the assessment, only a selected number of structures may warrant consideration for online review

(Smolders *et al* 2023a). Furthermore, the development of QA protocols that explicitly include information on dosimetric deviations is expected to increase the efficiency of contour reviewing. Some preliminary work have recently started to address this issue (Roberfroid *et al* 2024, Fankhauser *et al* 2024).

Furthermore, the possibility to incorporate DIR uncertainties into dose accumulation (Smolders *et al* 2023c, Amstutz *et al* 2021, Nenoff *et al* 2020) and to robustly optimize also against potential OAR propagation uncertainties (Smolders *et al* 2024, Nenoff *et al* 2022) will be crucial further steps to efficiently advance online adaptive treatment, even in the presence of deforming anatomy.

Our adaptive strategy is based on the online full optimization using a fast analytical dose calculation algorithm (Matter *et al* 2019). This approach offers two significant advantages: speed and the capacity to leverage favorable anatomical scenarios. Indeed, exploiting density heterogeneities and refined target-OAR separations, it is anticipated that, in the presence of deforming anatomy, full re-optimization outperforms alternative adaptive approaches such as dose restoration (Bernatowicz *et al* 2018, Miyazaki K *et al* 2023, Borderías *et al* 2022) or constrained re-optimization (Bobić *et al* 2023, Oud *et al* 2024), as it has been recently reported for head and neck patient.

A disadvantage of our strategy is however the need for daily full QA procedures. As described in appendix B and above, we have developed a comprehensive, rapid and automated QA procedure that guarantee safety without increasing the treatment time. The safety of the entire workflow, including the QA measures implemented, has been thoroughly evaluated by executing a Failure mode effect analysis (Czerska *et al* 2023) (details not reported here). In addition, we have developed a strategy to streamline the approval of the daily adapted plan by using DAPT-specific dose tolerances.

Another limitation of the DAPT workflow is the use of a fast but less accurate analytical dose calculation algorithm. However, the delivered dose can be accurately reconstructed retrospectively from log-files using a Monte Carlo algorithm. Therefore, the final treatment dose, as a record of what has been delivered, could be MC-based (Matter *et al* 2020). That is, the analytical dose calculation algorithm is only used as a fast surrogate in the online step, whereas the entire adaptive workflow could be considered MC-based from the point of view of dose accumulation and post-treatment plan review.

Looking ahead, our future efforts will focus on extending the DAPT capabilities to deformable anatomical regions and potentially integrating with commercial planning systems. This will further enhance the adaptability and effectiveness of our approach in treating a wider range of patients and anatomical variations.

5. Conclusion

In this work we have demonstrated the first ‘in-patient’ deliveries of a highly efficient DAPT workflow. Our study represents a pioneering use of online adaptation for proton therapy, paving the way for enhanced treatment precision.

Data availability statement

The data cannot be made publicly available upon publication because they contain sensitive personal information. The data that support the findings of this study are available upon reasonable request from the authors.

Acknowledgments

F Albertini would like to thank D Vaghini for the constant support during the development and clinical implementation phases and A Meijers for helpful critical discussions useful to refine the DAPT workflow. M Matter and L Nenoff have received funding from the Swiss National Science Foundation (SNSF) under the Grant Numbers SNF: 3200030_165961. E Choulilitsa and A Smolders have received funding from the European Union’s Horizon 2020 Marie Skłodowska-Curie Actions under Grant Agreement No. 955956. K Czerska has received funding from the European Union’s Horizon 2020 research and innovation program under the Marie Skłodowska-Curie Grant Agreement No. 884104 (PSI-FELLOW-III-3i) and the Krebsliga Grant (KFS-5660-08-2022). The authors have confirmed that any identifiable participants in this study have given their consent for publication.

Conflict of interest

The authors declare that they have no competing interest.

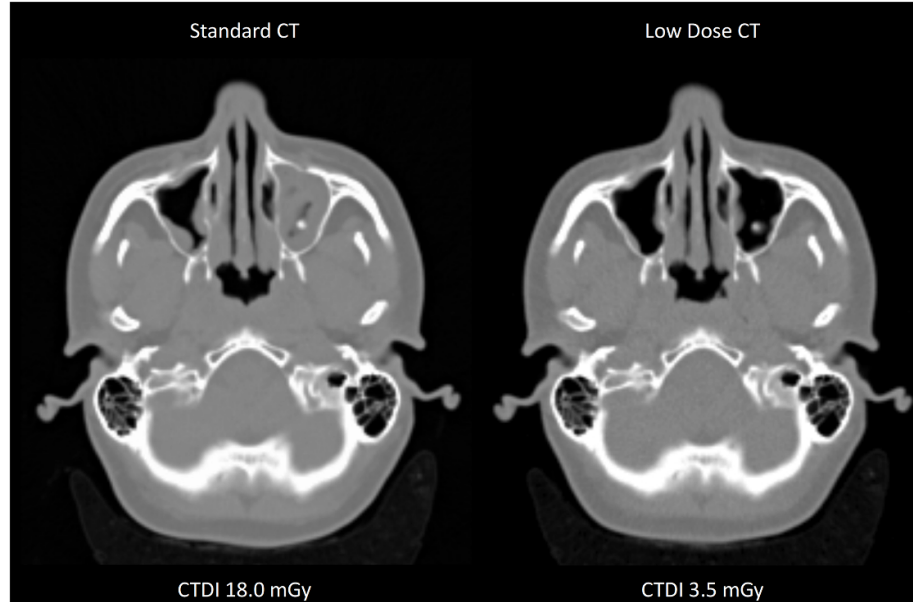


Figure 7. Comparison of the planning CT (using the standard CT protocol) and a daily CT (using the low-dose CT protocol) for one of the DAPT patients. The daily CT is slightly more noisy than the planning CT, but this has minimal dosimetric impact.

Appendix A. Low-Dose CT

A dedicated low-dose CT protocol has been defined with the aim of reducing the imaging dose, while not affecting the dose calculation. To identify the optimal parameters, images with varying settings were acquired for both an anthropomorphic phantom and an electron density phantom (CIRS) (Nenoff *et al* 2021). Variations in HUs were evaluated across these settings. Moreover, a 3 field IMPT plan was optimized on each low-dose CT and compared to the same plan reoptimized on the diagnostic CT. This study resulted in the introduction of a low-dose protocol (120 kV, quality reference mAs: 20, care dose, pitch 1, rotation time 0.5 s) that reduces the CTDI by approximately one third and cuts the acquisition time by 50% compared to the standard protocol (120 kV, quality reference mAs: 320, care dose, pitch 0.6, rotation time 1 s). The calibration curve was defined similarly as for the planning CT as described elsewhere (Schneider *et al* 1996). The protocol was recently experimentally revalidated by subsequently acquiring a diagnostic and 5 low-dose CT scans of an anthropomorphic phantom. A 4-field treatment plan was optimized on each low-dose CT and compared to the same plan reoptimized on the diagnostic CT. In all cases, the 2%/2 mm gamma pass rate in the body was above 99.9%, justifying the use of the low-dose CT protocol for daily plan reoptimization. Figure 7 provides an example of images acquired with both the clinical standard and the new low-dose protocols.

Appendix B. Online QA process for DAPT

We have identified a set of automatic QA checks to support the online approval of the DAPT workflow. All described checks compare a specific metric, derived from the daily plan, to expected values. These expected values are extended with clinically acceptable thresholds for which the QA check will fail if violated. For this work, all thresholds have been defined based on an analysis of a comprehensive set of clinically delivered and validated patient plans and treatments.

Structure propagation

To QA the automatic structure propagation, the following checks have been defined:

- Check that the volume of each structure remains consistent with the template plan
- Check that the HU values inside ad-hoc defined ‘control QA structures’ are consistent with the template plan
- Consistency of HU values between the reference CT and the daily CT
- Check that the change of the center of mass point between the reference and the propagated structures is consistent with the geometric transformation defined by the rigid registration

Table 5. Example of QA checks performed.

Center of Mass [mm]	Difference	Threshold	Check		
CTV	0.2	1			Passed
Brainstem	0.1	1			Passed
Chiasm	0.3	1			Passed
Optic nerve right	0.9	1			Passed
Volume [cm ³]	Template	Daily	Difference	Threshold	Check
CTV	15.36	15.14	0.22cm ³	1cm ³	Passed
Brainstem	27.4	27.56	0.16cm ³	1cm ³	Passed
Chiasm	0.43	0.40	6.9%	30%	Passed
Optic nerve right	0.47	0.44	6.3%	30%	Passed
Mean HU above lowest 15% [HU]	Template	Daily	Difference	Threshold	Check
Control structure 1	1235	1239	-4	200	Passed
Control structure 2	1408	1379	29	200	Passed
Control structure 3	1453	1450	3	200	Passed
CT congruency	Diff	Threshold	Check		
CT RMS difference [HU]	192	300			Passed

Control QA structures are contoured on the planning CT in proximity to the target volume. These include clearly defined bony structures which are expected not to move in relation to the target volume.

The MD is responsible to give the final approval of the daily structures. If the structure QA fails, daily contours should be manually adjusted.

Clinical dose assessment

Similar to the pre-treatment evaluation, the clinical acceptance of the daily plan must be rigorously assessed. Efficiency in this evaluation process is achieved by establishing decision-making criteria during the pre-treatment phase. This groundwork is documented in the DAPT daily acceptance table, defined by the responsible medical doctor after the approval of the template plan. For each relevant clinical goals for Organ At Risk (OAR) and target DVH, acceptable variations from those achieved in the template plan are specified. A daily difference of 5% (corresponding to a difference of 0.1 Gy_RBE per fraction, for a delivered dose of 2Gy_RBE/fr) is generally considered clinically acceptable. Tighter tolerances have been defined for individual OARs as per MD request.

These variations aid in evaluating the validity of the automatically generated daily plan, employing a traffic light protocol with the following color scheme:

- Green: Indicates a value equal to or better than accepted in the template plan.
- Yellow: Represents a value worse than the template plan, yet within the specified tolerance.
- Red: Indicates a value worse than the accepted template value, exceeding the defined tolerance.

In addition, alongside the clinical goals evaluations utilizing the traffic light protocol, the clinical assessment also include a visual evaluation of the daily-adapted plan optimized on the daily anatomy and DVHs comparisons of critical volumes between the template and the daily adapted plan. An illustration of the clinical evaluation can be seen in figure 5(d) in the main text.

Plan QA

The plan QA checks encompass the following:

- Dose reconstruction from machine control files
- Machine file comparison

An example of the performed checks is shown in table 6.

In the first step after the daily plan generation, a machine control file, which contains all machine parameters relevant for delivery of the fraction, is generated. This contains all pencil beam positions and fluences, but also the order in which the pencil beams will be applied, the magnet ramping sequences at the start of each field and all patient couch motions. Since the machine file contains all information relevant for

Table 6. Example of Plan QA checks performed.

Dose reconstruction from machine file	Value	Threshold	Check			
Integrity check:	0.12%	1%	Passed			
Max voxel difference [%]						
Independent Dose Calculation (IDC):	99.95%	95%	Passed			
Voxel passing γ analysis (3%/3 mm)						
Machine File comparison	Equal	Template	Daily	Difference [%]	Threshold [%]	Check
Patient data	true					Passed
Number of fields	true					Passed
Settings field 1	true					Passed
Settings field 2	true					Passed
Number of spots field 1	5173	5084	1.72	10		Passed
Number of spots field 2	5945	5970	0.42	10		Passed
Max energy field 1 [keV]	146 604	146 604	0.00	5		Passed
Max energy field 2 [keV]	127 728	129 208	1.16	5		Passed
Total MU field 1	2207 171	2208 832	0.08	10		Passed
Total MU field 2	3072 566	2881 157	6.23	10		Passed

the treatment, this is used to recalculate the dose distribution on the daily CT using an independent implementation of the same dose calculation algorithm (Schneider *et al* 1996). The resulting recomputed dose is automatically compared to the initially planned dose. This approach was shown to have a higher sensitivity for the detection of errors in the data transfer or data processing than patient specific verification measurements (Meier *et al* 2015). If differences between this reconstructed dose and the daily plan exceed the tolerance threshold (< 1% voxel dose difference over all voxels), as derived for a set of clinical cases by Matter *et al* (2015), this check fails.

It is important that an independent implementation of the same dose calculation algorithm as used for calculation of the template and daily plan (i.e. Raycasting) is used for dose reconstruction to test the integrity of the machine file.

In addition, during offline dose review, a second dose reconstruction is performed, which is based on delivery log-files and the use of a completely independent Monte Carlo dose calculation (Meier *et al* 2015). Thus, a comprehensive assessment of the accuracy of the dose calculation and delivery is ultimately performed as part of the offline review process. A gamma passing rate above 95% (for 3%/3mm tolerances) indicates a good agreement between the planned and the delivered dose.

In addition to these checks, sanity assessments are conducted by comparing machine files of template and daily adapted plans. As the daily plan should generally be very similar to the template plan (i.e. only adapted for density changes) the machine control files should also be similar. The machine file for the template plan underwent the full patient specific quality assurance procedures, including measurements (Lomax *et al* 2004). Various metrics such as patient ID, spot and monitor unit (MU) counts, field parameters, and energy are evaluated. This evaluation employs a pass-and-fail traffic light protocol for assessment. Thresholds were derived by analyzing deviations in machine files for a set of clinical cases re-optimized on control CTs acquired during the treatment. An example of the performed checks is shown in table 6.

Discussion

The set of proposed QA checks for both structure propagation and plan QA presented here merged from careful considerations about potential errors in the workflow. Everything except the actual spot list is identical to the verified template plan. This is verified during the comparison of the machine control files of the template and daily plans. In addition, the total number of spots and total number of monitor units are only allowed to deviate a certain amount from the template machine file. Obviously, the new spot list results in a new dose distribution, which is verified by dose reconstructions based on the machine control file. This is a proven QA tool which has been used clinically at our institute for many years (Lomax *et al* 2004). In addition, the clinical dose distribution is assessed both visually and by evaluating variations in the achieved clinical goals. As such, the whole procedure represents a comprehensive online QA for DAPT.

Appendix C. Dose metrics for the individual patients

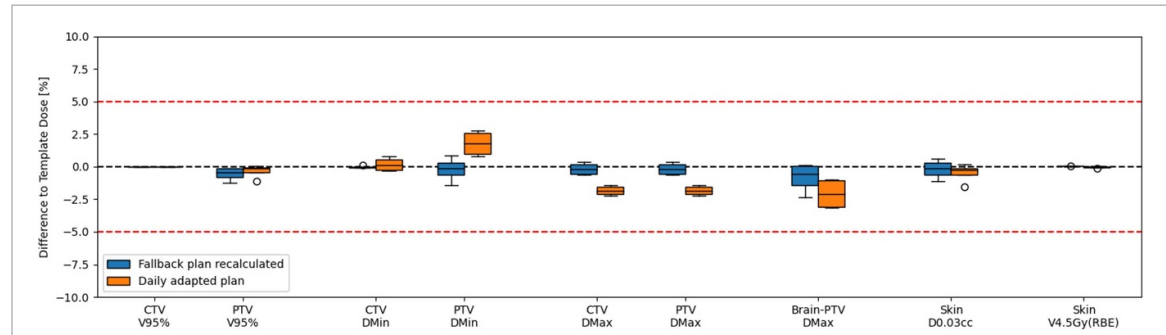


Figure 8. Deviations in daily dose metrics from the planned value for both the fallback and adapted plans for patient 1.

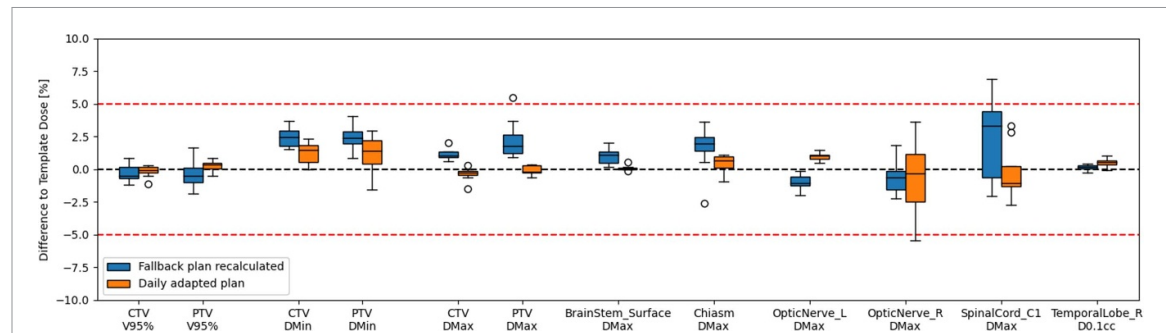


Figure 9. Deviations in daily dose metrics from the planned value for both the fallback and adapted plans for patient 2.

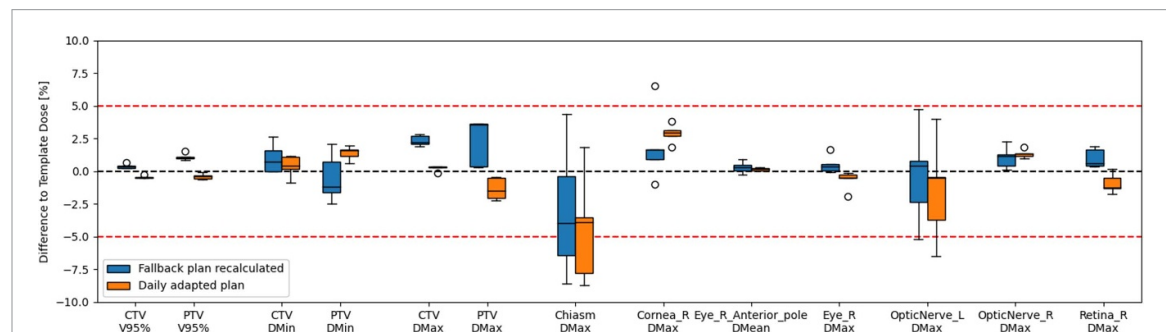


Figure 10. Deviations in daily dose metrics from the planned value for both the fallback and adapted plans for patient 3.

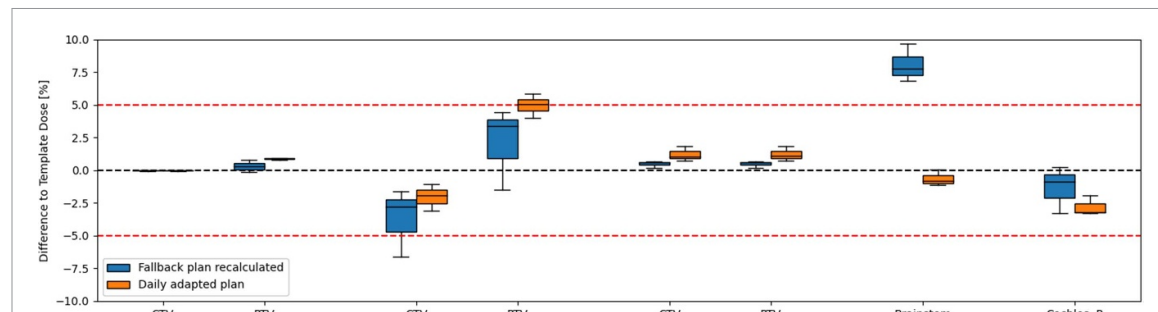


Figure 11. Deviations in daily dose metrics from the planned value for both the fallback and adapted plans for patient 4.

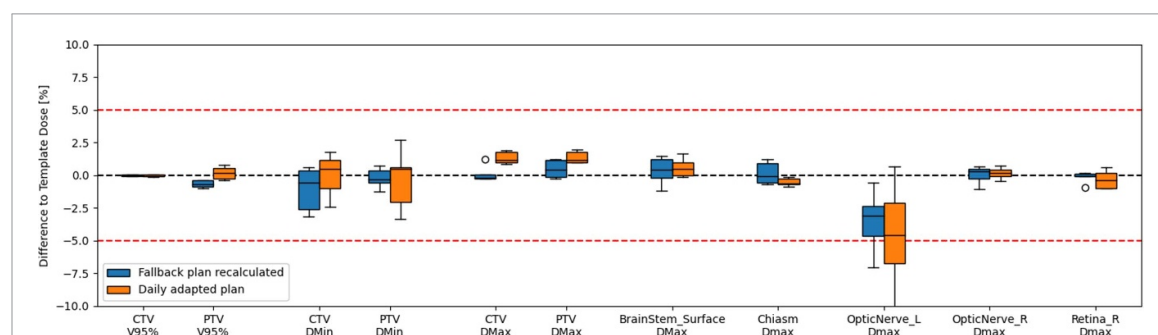


Figure 12. Deviations in daily dose metrics from the planned value for both the fallback and adapted plans for patient 5.

ORCID iDs

F Albertini <https://orcid.org/0000-0002-2547-1269>
E Choullilitsa <https://orcid.org/0009-0004-4940-9680>
A Smolders <https://orcid.org/0000-0003-2874-3634>

References

- Acharya S *et al* 2016 Online magnetic resonance image guided adaptive radiation therapy: first clinical applications *Int. J. Radiat. Oncol.* **94** 394–403
- Albertini F *et al* 2015 PO-1000: first year of clinical experience with the new generation of Gantry for active scanning proton therapy *Radiat. Oncol.* **115** S536
- Albertini F, Matter M, Nenoff L, Zhang Y and Lomax A 2020 Online daily adaptive proton therapy *Br. J. Radiol.* **93** 20190594
- Amstutz F, Nenoff L, Albertini F, Ribeiro C O, Knopf A C, Unkelbach J, Weber D C, Lomax A J and Zhang Y 2021 An approach for estimating dosimetric uncertainties in deformable dose accumulation in pencil beam scanning proton therapy for lung cancer *Phys. Med. Biol.* **66** 105007
- Belosi M F, van der Meer R, García de Acilu Laa P, Bolsi A, Weber D C and Lomax A J 2017 Treatment log files as a tool to identify treatment plan sensitivity to inaccuracies in scanned proton beam delivery *Radiat. Oncol.* **125** 514–9
- Bernatowicz K, Geets X, Barragan A, Janssens G, Souris K and Sterpin E 2018 Feasibility of online IMPT adaptation using fast, automatic and robust dose restoration *Phys. Med. Biol.* **63** 085018
- Bobić M *et al* 2023 Large anatomical changes in head-and-neck cancers—a dosimetric comparison of online and offline adaptive proton therapy *Clin. Transl. Radiat. Oncol.* **40** 100625
- Borderías-Villarroel E, Taasti V, Van Elmpt W, Teruel-Rivas S, Geets X and Sterpin E 2022 Evaluation of the clinical value of automatic online dose restoration for adaptive proton therapy of head and neck cancer *Radiat. Oncol.* **170** 190–7
- Bortfeld T and Paganetti H 2006 The biologic relevance of daily dose variations in adaptive treatment planning *Int. J. Radiat. Oncol.* **65** 899–906
- Byrne M *et al* 2022 Varian ethos online adaptive radiotherapy for prostate cancer: early results of contouring accuracy, treatment plan quality, and treatment time *J. Appl. Clin. Med. Phys.* **23** e13479
- Chang C, Bohannon D, Tian Z, Wang Y, McDonald M W, Yu D S, Liu T, Zhou J and Yang X 2024 A retrospective study on the investigation of potential dosimetric benefits of online adaptive proton therapy for head and neck cancer *J. Appl. Clin. Med. Phys.* **25** e14308
- Cubillo-Mesías M, Troost E G C, Lohaus F, Agolli L, Rehm M, Richter C and Stützer K 2019 Including anatomical variations in robust optimization for head and neck proton therapy can reduce the need of adaptation *Radiat. Oncol.* **131** 127–34
- Czerska K *et al* 2023 Use of failure mode and effects analysis to efficiently implement daily adaptive proton therapy workflow in the clinic *Conf. Proc. PTCOG*
- Fankhauser L S, Smolders A, Bellotti R, Weber D C, Lomax A J and Albertini F 2024 Automatic contour quality assurance (CAT-QA) to speed up online adaptive radiotherapy *Conf. Proc. ICCR*

- Glide-Hurst C K *et al* 2021 Adaptive radiation therapy (ART) strategies and technical considerations: a state of the ART review from NRG oncology *Int. J. Radiat. Oncol.* **109** 1054–75
- Güngör G *et al* 0000 Report Time Analysis of Online Adaptive Magnetic Resonance Guided Radiation Therapy Workflow According to Anatomical Sites (<https://doi.org/10.1016/j.prro.2020.07.003>)
- Jagt T Z, Breedveld S, van Haveren R, Heijmen B J M and Hoogeman M S 2020 Online-adaptive versus robust IMPT for prostate cancer: how much can we gain? *Radiat. Oncol.* **151** 228–33
- Janson M, Glimelius L, Fredriksson A, Traneus E and Engwall E 2024 Treatment planning of scanned proton beams in RayStation *Med. Dosim.* **49** 2–12
- Korevaar E W *et al* 2019 Practical robustness evaluation in radiotherapy—a photon and proton-proof alternative to PTV-based plan evaluation *Radiat. Oncol.* **141** 267–74
- Lalonde A, Bobić M, Sharp G C, Chamseddine I, Winey B and Paganetti H 2023 Evaluating the effect of setup uncertainty reduction and adaptation to geometric changes on normal tissue complication probability using online adaptive head and neck intensity-modulated proton therapy *Phys. Med. Biol.* **68** 115018
- Lalonde A, Bobić M, Winey B, Verburg J, Sharp G C and Paganetti H 2021 Anatomic changes in head and neck intensity-modulated proton therapy: comparison between robust optimization and online adaptation *Radiat. Oncol.* **159** 39–47
- Li B, Lee H C, Duan X, Shen C, Zhou L, Jia X and Yang M 2017 Comprehensive analysis of proton range uncertainties related to stopping-power-ratio estimation using dual-energy CT imaging *Phys. Med. Biol.* **62** 7056–74
- Lomax A J *et al* 2004 Treatment planning and verification of proton therapy using spot scanning: initial experiences *Med. Phys.* **31** 3150–7
- Lomax A J 2008 Intensity modulated proton therapy and its sensitivity to treatment uncertainties 2: the potential effects of inter-fraction and inter-field motions *Phys. Med. Biol.* **53** 1043–56
- Lomax A 1999 Intensity modulation methods for proton radiotherapy *Phys. Med. Biol.* **44** 185–205
- Lomax J A *et al* 1996 A 3D treatment planning for conformal proton therapy by spot scanning *Quantitative Imaging in Oncology* (available at: www.scienceopen.com/document?vid=3e3a597b-4c23-45c6-853a-7511022d3a34) (Accessed 18 December 2017)
- Matter M 2020 Technical Implementation of Daily Adaptive Proton Therapy **10.3929/ethz-b-000460899**
- Matter M, Nenoff L, Marc L, Weber D C, Lomax A J and Albertini F 2020 Update on yesterday's dose—Use of delivery log-files for daily adaptive proton therapy (DAPT) *Phys. Med. Biol.* **65** 195011
- Matter M, Nenoff L, Meier G, Weber D C, Lomax A J and Albertini F 2018 Alternatives to patient specific verification measurements in proton therapy: a comparative experimental study with intentional errors *Phys. Med. Biol.* **63** 205014
- Matter M, Nenoff L, Meier G, Weber D C, Lomax A J and Albertini F 2019 Intensity modulated proton therapy plan generation in under ten seconds *Acta Oncol.* **58** 1435–9
- Meier G, Besson R, Nanz A, Safai S and Lomax A J 2015 Independent dose calculations for commissioning, quality assurance and dose reconstruction of PBS proton therapy *Phys. Med. Biol.* **60** 2819–36
- Miyazaki K *et al* 2023 Deformed dose restoration to account for tumor deformation and position changes for adaptive proton therapy *Med. Phys.* **50** 675–87
- Nenoff L *et al* 2020 Deformable image registration uncertainty for inter-fractional dose accumulation of lung cancer proton therapy Radiotherapy and Oncology **147** 178–185
- Nenoff L, Buti G, Bobić M, Lalonde A, Nesteruk K P, Winey B, Sharp G C, Sudhyadhom A and Paganetti H 2022 Integrating structure propagation uncertainties in the optimization of online adaptive proton therapy plans *Cancers* **14** 3926
- Nenoff L, Matter M, Charmillot M, Krier S, Uher K, Weber D C, Lomax A J and Albertini F 2021 Experimental validation of daily adaptive proton therapy *Phys. Med. Biol.* **66** 205010
- Nenoff L, Matter M, Hedlund Lindmar J, Weber D C, Lomax A J and Albertini F 2019 Daily adaptive proton therapy—the key to innovative planning approaches for paranasal cancer treatments *Acta Oncol.* **58** 1423–8
- Oud M, Breedveld S, Rojo-Santiago J, Giżyńska M K, Kroesen M, Habraken S, Perkó Z, Heijmen B and Hoogeman M 2024 A fast and robust constraint-based online re-optimization approach for automated online adaptive intensity modulated proton therapy in head and neck cancer *Phys. Med. Biol.* **69** 075007
- Paganetti H 2012 Range uncertainties in proton therapy and the role of Monte Carlo simulations *Phys. Med. Biol.* **57** R99–R117
- Paganetti H *et al* 2021 Roadmap: proton therapy physics and biology *Phys. Med. Biol.* **66** 05RM01
- Paganetti H, Botas P, Sharp G C and Winey B 2021 Adaptive proton therapy *Phys. Med. Biol.* **66** 22TR01
- Papalazarou C, Klop G J, Milder M T W, Marijnissen J P A, Gupta V, Heijmen B J M, Nuyttens J J M E and Hoogeman M S 2017 CyberKnife with integrated CT -on-rails: system description and first clinical application for pancreas SBRT *Med. Phys.* **44** 4816–27
- Pedroni E *et al* 2004 The PSI Gantry 2: a second generation proton scanning gantry *Orig. Z. Med. Phys.* **14** 25–34
- Pedroni E, Meer D, Bula C, Safai S and Zenklusen S 2011 Pencil beam characteristics of the next-generation proton scanning gantry of PSI: design issues and initial commissioning results *Eur. Phys. J. Plus* **126** 1–27
- Peters N, Wohlfahrt P, Hofmann C, Möhler C, Menkel S, Tschiche M, Krause M, Troost E G C, Enghardt W and Richter C 2022 Reduction of clinical safety margins in proton therapy enabled by the clinical implementation of dual-energy CT for direct stopping-power prediction *Radiat. Oncol.* **166** 71–78
- PTCOG 2024 PTCOG website (available at: www.ptcog.site/)
- Raaymakers B W *et al* 2017 First patients treated with a 1.5 T MRI-Linac: clinical proof of concept of a high-precision, high-field MRI guided radiotherapy treatment *Phys. Med. Biol.* **62** L41–L50
- Roberfroid B, Lee J A, Geets X, Sterpin E and Barragán-Montero A M 2024 DIVE-ART: a tool to guide clinicians towards dosimetrically informed volume editions of automatically segmented volumes in adaptive radiation therapy *Radiat. Oncol.* **192** 110108
- Scandurra D, Albertini F, van der Meer R, Meier G, Weber D C, Bolsi A and Lomax A 2016 Assessing the quality of proton PBS treatment delivery using machine log files: comprehensive analysis of clinical treatments delivered at PSI Gantry 2 *Phys. Med. Biol.* **61** 1171
- Schaffner B, Pedroni E and Lomax A 1999 Dose calculation models for proton treatment planning using a dynamic beam delivery system: an attempt to include density heterogeneity effects in the analytical dose calculation *Phys. Med. Biol.* **44** 27–41
- Schiavi A, Senzacqua M, Pioli S, Mairani A, Magro G, Molinelli S, Ciocca M, Battistoni G and Patera V 2017 Fred: a GPU-accelerated fast-Monte Carlo code for rapid treatment plan recalculations in ion beam therapy *Phys. Med. Biol.* **62** 7482–504
- Schneider U, Pedroni E and Lomax A 1996 The calibration of CT Hounsfield units for radiotherapy treatment planning *Phys. Med. Biol.* **41** 111
- Smolders A *et al* 2024 Robust optimization strategies for contouring uncertainties in online adaptive radiation therapy *Phys. Med. Biol.* **69** 165001

- Smolders A, Choullitsa E, Czerska K, Bizzocchi N, Krcek R, Lomax A, Weber D C and Albertini F 2023a Dosimetric comparison of autocontouring techniques for online adaptive proton therapy *Phys. Med. Biol.* **68** 175006
- Smolders A, Hengeveld A C, Both S, Wijsman R, Langendijk J A, Weber D C, Lomax A J, Albertini F and Guterres Marmitt G 2023b Inter- and intrafractional 4D dose accumulation for evaluating Δ NTCP robustness in lung cancer *Radiat. Oncol.* **182** 109488
- Smolders A, Lomax A, Weber D C and Albertini F 2023c Deep learning based uncertainty prediction of deformable image registration for contour propagation and dose accumulation in online adaptive radiotherapy *Phys. Med. Biol.* **68** 245027
- Taasti V T et al 2023 Clinical benefit of range uncertainty reduction in proton treatment planning based on dual-energy CT for neuro-oncological patients *Br. J. Radiol.* **96** 1149
- Unkelbach J et al 2018 Robust radiotherapy planning *Phys. Med. Biol.* **63** 22TR02
- van Herk M, McWilliam A, Dubec M, Faivre-Finn C and Choudhury A 2018 Magnetic resonance imaging-guided radiation therapy: a short strengths, weaknesses, opportunities, and threats analysis *Int. J. Radiat. Oncol.* **101** 1057–60
- Werenstein-Honingh A M et al 2019 Feasibility of stereotactic radiotherapy using a 1.5 T MR-linac: multi-fraction treatment of pelvic lymph node oligometastases *Radiat. Oncol.* **134** 50–54
- Winkel D et al 2019 Adaptive radiotherapy: the Elekta Unity MR-linac concept *Clin. Transl. Radiat. Oncol.* **18** 54–59
- Winterhalter C, Meier G, Oxley D, Weber D C, Lomax A J and Safai S 2019 Log file based Monte Carlo calculations for proton pencil beam scanning therapy *Phys. Med. Biol.* **64** 035014
- Yan D, Vicini F, Wong J and Martinez A 1997 Adaptive radiation therapy *Phys. Med. Biol.* **42** 123–32